Improvement of a bidimensional overset structured mesh generation and adaptation method, based on a near-body/off-body partitioning

E. Kultajev[1], C. Benoit[1], S. Peron[1], and A. Lerat[2]

[1] Onera - The French Aerospace Lab, F-92322 Châtillon, France,
`ekaterina.kultajev@onera.fr`, `christophe.benoit@onera.fr`,
`stephanie.peron@onera.fr`
[2] DynFluid Lab., Arts et Métiers ParisTech, Paris, France, `alain.lerat@ensam.eu`

An automatic overset structured mesh generation and adaptation method for Computational Fluid Dynamics (CFD) is being developed at Onera. This method is based on computational domain partitioning into off-body Cartesian regions and near-body curvilinear regions [1] and has been introduced to simplify the mesh generation process. Off-body grids are a set of structured Cartesian grids that can be automatically generated and adapted [1, 2]. The Chimera method enables solution transfer between grids [3, 4, 5].
Previously, a method based on geometry decomposition identifying sharp edges has been developed to automatically generate short extension near-body grids around bidimensional geometries with a regular step along the wall [6]. Here we describe an extension of this method, generating non-uniform, curvature-dependent and flow features-dependent grid step along the wall.
Keywords: mesh generation, mesh adaptation, structured mesh, overset grids.

1 Adaptation of near-body grids to curvature

The overset near-body grids are directly build from the CAD curve data, which is mapped with a small uniform point distribution. The discretized curve is split into a set of curves at points presenting sharp edges. We use cubic spline interpolation to remap each curve with a curvature-dependent distribution, so that the grid spacing along the wall is proportional to the curvature radius of the curve, bounded by minimum and maximum spacing values. Short extension grids are then generated as described in [6].
A non-uniform distribution along the wall has two main advantages: it can be curvature-dependent thus enhancing accuracy on the leading edge of an airfoil (Fig. 1(a)); it makes also possible the meshing around a body with small-scale details, such as an airfoil with a truncated trailing edge (Fig. 1(b)-1(c)).
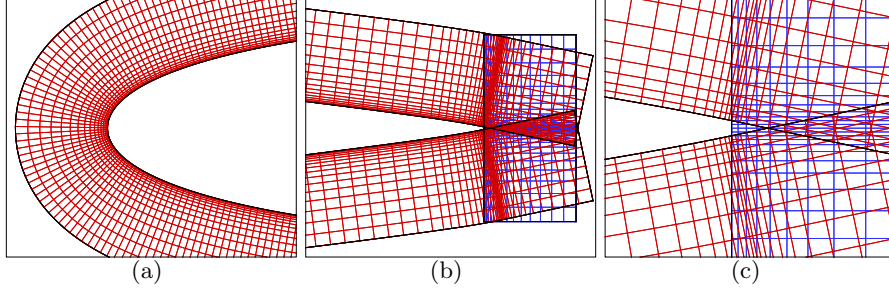
Fig. 1. (a) Curvature-dependent distribution on a leading edge; (b) truncated trailing edge; (c) close-up view.

2 Adaptation of near-body grids to flow solution

After a first CFD computation on an automatically generated mesh with curvature-dependent near-body grids and consistent off-body grids in terms of cell size, the mesh can be adapted to the flow solution in order to improve the accuracy. After a first computation on the initial mesh, the off-body Cartesian mesh is adapted according to an adaptation sensor based on flow features [2]. This sensor is then used to generate new near-body grids with curvature-dependent and sensor-dependent distributions. The grid spacing is either proportional to the curvature radius or inversely proportional to the sensor, whichever is smaller (with appropriate bounds). A flow simulation is then performed on the adapted mesh, using the interpolated solution from the previous computation as initial condition. This adaptation process can be repeated as many times as needed.

3 Results

The method has been validated on a RANS flow simulation past a RAE2822 airfoil and on an inviscid flow simulation past a NACA0012 airfoil. Solutions are compared to those obtained on single-block C-type meshes.

3.1 RANS transsonic flow simulation past a RAE2822 airfoil

First we consider a RANS flow simulation past a RAE2822 airfoil with an angle of attack of 2.79 degrees, a Reynolds number of $6.5.10^6$, and a freestream Mach number of 0.73. The RANS equations are solved by a 2nd-order space-centered Jameson Finite-Volume scheme [7], with a scalar artificial dissipation ($k_2 = 1.$, $k_4 = 0.032$). The time integration scheme is the implicit backward Euler scheme, with a CFL number of 100. The turbulence model is the Wilcox $k - \omega$ model [8].

The single-block mesh, manually refined in the shock area, and the automatic mesh contain respectively 103,113 and 517,345 points (Fig. 2). We choose the parameters of automatic mesh generation and adaptation such that the points distribution along the wall is close to the one on the single-block mesh. As expected, the near-body mesh refines in the shock area. Pressure coefficient on the wall and skin friction coefficient are displayed on figure 3. The shock is well captured, although some fluctuations are observed at the leading edge. This is because the remapping of the airfoil causes errors, since the original airfoil definition is discrete and contains few points.
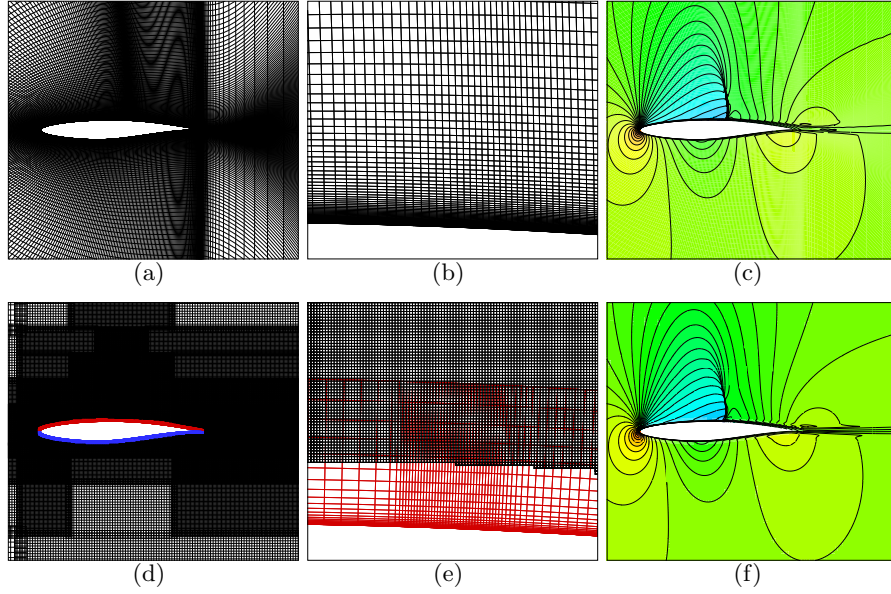

Fig. 2. RAE2822 airfoil: (a-b-c) single-block mesh; (b) close-up view in the vicinity of the shock; (c) isodensity contours; (d-e-f) automatic mesh; (e) close-up view in the vicinity of the shock; (f) isodensity contours.
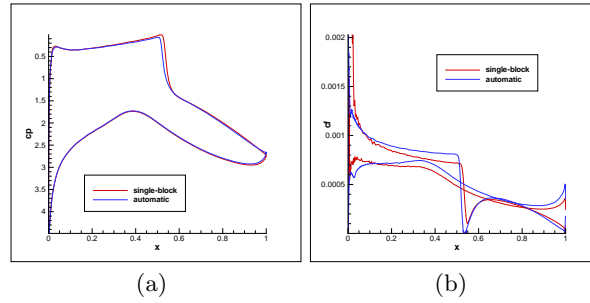

Fig. 3. RAE2822 airfoil: (a) pressure coefficient on wall; (b) skin friction coefficient.

3.2 Inviscid transsonic flow simulation past a NACA0012 airfoil

In order to avoid the above problem, we considered an inviscid flow simulation past a NACA0012 airfoil with an angle of attack of 1 degree and a freestream Mach number of 0.86. The Euler equations are solved by a Roe Finite-Volume scheme [9]. The time integration scheme is the implicit backward Euler scheme, with a CFL number of 30.
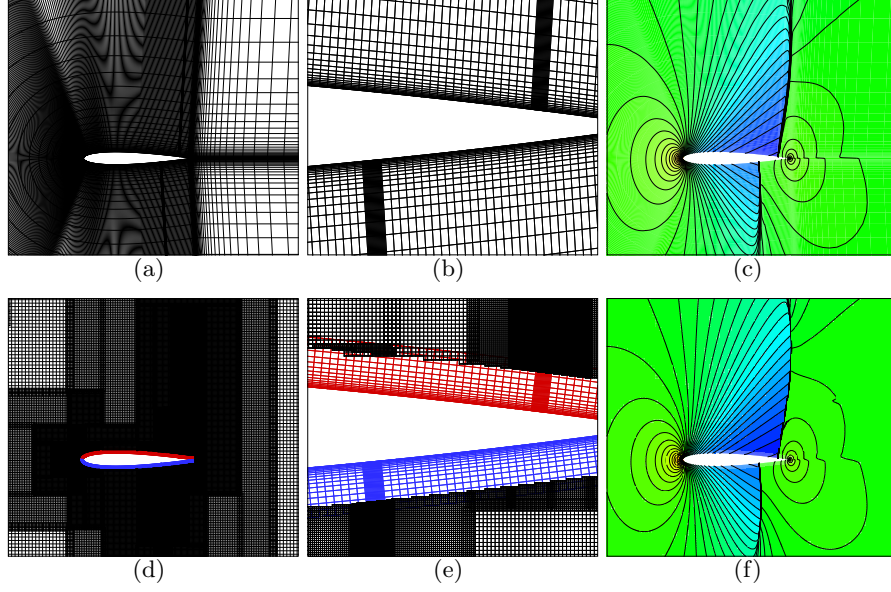

(a)   (b)   (c)

(d)   (e)   (f)

Fig. 4. NACA0012 airfoil: (a-b-c) single-block mesh; (b) close-up view in the vicinity of shocks; (c) isodensity contours; (d-e-f) automatic mesh; (e) close-up view in the vicinity of shocks; (f) isodensity contours.
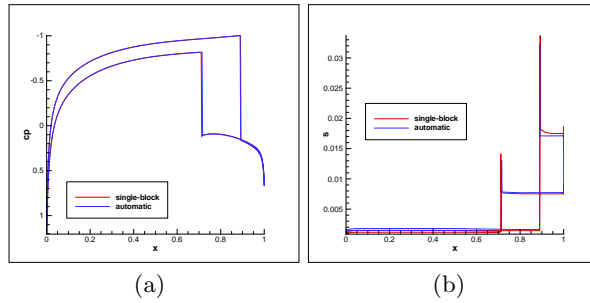

(a)   (b)

Fig. 5. NACA0012 airfoil: (a) pressure coefficient on wall; (b) entropy on wall.

The single-block and the automatic meshes contain respectively 31,050 and 475,410 points (Fig. 4). The points distribution along the wall on the single-block mesh is the same as on the automatic one. Note that on the automatic mesh the shock is better captured away from the wall, since the off-body mesh adaptation follows the shock structure, whereas for the single-block mesh, the shock falls out of the refined region. Pressure coefficient and entropy on the wall are displayed on figure 5, showing very similar results.

4 Conclusion

The work presented here is an improvement to an existing automatic overset structured mesh generation and adaptation method. It allows to automatically generate near-body meshes with a non-uniform distribution along the wall and therefore making curvature-dependent or flow features-dependent distributions. It has been validated on a RANS transsonic flow simulation past a RAE2822 airfoil and on an inviscid transsonic flow simulation past a NACA0012 airfoil with promising results.

References

1. Meakin RL (2000) Adaptive Spatial Partitioning and Refinement for Overset Structured Grids. Computer Methods in Applied Mechanics and Engineering 2000; 189:1077-1117
2. Peron S, Benoit C (2011) Automatic off-body overset adaptive Cartesian mesh method based on an octree approach. AIAA Paper 2011-3050
3. Benek JA, Steger JL, Dougherty FC (1983) A Flexible Grid Embedding Technique with Application to the Euler Equations. AIAA Paper 83-1944
4. Peron S, Benoit C (2010) Development of a Python Preprocessing Module for Chimera Assembly for CFD Applications. 2010 Overset Grid Symposium
5. Suhs NE, Rogers SE, Dietz WE (2002) PEGASUS 5: An Automated Pre-Processor for Overset-Grid CFD. AIAA Paper 2002-3186
6. Benoit C, Crochepeyre FL, Jeanfaivre G, Peron S (2009) Développement d'une technique de génération automatique de maillages recouvrants cartésiens/curvilignes. Génération automatique de grilles de corps. Tech. Rep. RT 1/13752 DSNA, ONERA
7. Jameson A, Schmidt W, Turkel E (1981) Numerical Solutions of the Euler Equations by Finite Volume Methods Using Runge-Kutta Time Stepping. AIAA Paper 81-1259
8. Wilcox DC (1988) Simulation of transition with a two-equation turbulence model. AIAA Journal 26(11):1299-1310
9. Roe PL (1981) Approximate Riemann solvers, parameter vectors, and difference schemes. Journal of Computational Physics 43(2):357-372